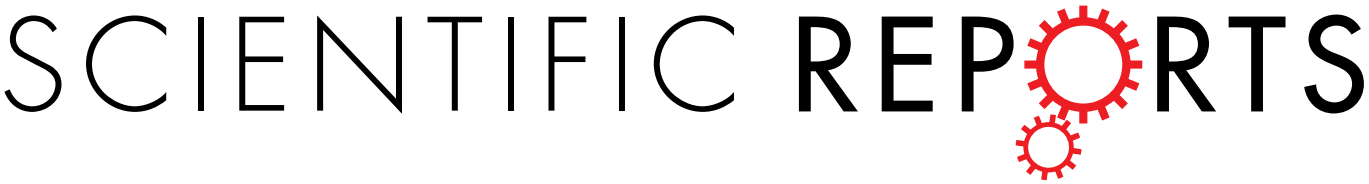

OPEN

Inorganic carbon distribution and CO_2 fluxes in a large European estuary (Tagus, Portugal)

Received: 15 May 2015
Accepted: 14 June 2017
Published online: 07 August 2017

A. P. Oliveira[1,2], G. Cabeçadas[1] & M. D. Mateus[3]

Ten field cruises were carried out in Tagus estuary from 1999 to 2007 to study the dynamics of the inorganic carbon system. Dissolved inorganic carbon (DIC) and total alkalinity (TA) increased with salinity. DIC and TA were generally conservative in the estuarine mixing zone (salinity >10), while a complex distribution pattern was observed at the upper estuary. DIC values peaked 1786.9 ± 155.8 µmol kg^{-1} at that segment. Estimated annual mean fluxes of DIC were 0.27 Tg C yr^{-1} from the river to the estuary, and 0.37 Tg C yr^{-1} from here to the coastal area. The Tagus estuary was always CO_2 supersaturated, with partial pressure of CO_2 (pCO_2) reaching 9160 µatm in the upper estuary. An average emission of 0.11 Tg C yr^{-1} was estimated from the estuary to the atmosphere, corresponding to 23% of exported DIC. Only 8% of the riverine DIC was ventilated. The non-conservative behaviour of CO_2 parameters in the estuary segment under freshwater influence was attributed to alternations in the relevance of riverine/terrestrial runoff, photosynthesis, aerobic respiration, organic matter mineralization and $CaCO_3$ precipitation/dissolution.

Estuaries rank among the most productive and dynamic aquatic ecosystems[1]. They are frequently characterized by strong physical-chemical gradients, enhanced biological activity and intense sediment dynamics. Nowadays it is unequivocally accepted that inner estuaries act as sources of CO_2 to the atmosphere. A recent study[2] reports that estuaries emit 20.8 mol C m^{-2} yr^{-1} to the atmosphere, mainly due to their heterotrophic metabolic status, sustained by terrestrial/riverine organic carbon inputs, and also by waste water in populated areas. A fraction of this carbon is exported to the nearby coastal areas mostly as organic particles, but also to the atmosphere in the form of CO_2 emissions. Hence, inner estuaries are effective sieves for terrestrial/riverine inputs and provide a by-pass of carbon towards the atmosphere[3].

The flux and/or residence of carbon in each of these compartments depend on the characteristics of the estuary, as well as on the season, and even time of day. For example, approximately 60% of the respiratory CO_2 in Scheldt estuary is released to the atmosphere, 26% transferred to the sediment, and only 14% remains in the water column[1]. Moreover, spatial variability plays an important role due to the hydrodynamic and geomorphological complexity of these littoral zones. Thus, fluxes, sources and mechanisms of CO_2 transport and transformation are among the most important current issues in marine and freshwater geochemistry.

A compilation[4] of available data on water-air CO_2 fluxes in inner estuaries shows that the west European inner estuaries have been extensively studied, accounting for 47% of the total results presented. So far, inter-annual and decadal variability of water-air CO_2 fluxes is still undocumented in some estuarine environments. Few studies have been undertaken involving CO_2 fluxes variability in Portugal, a country at the eastern boundary of the Subtropical North Atlantic. Data of water-air CO_2 fluxes are available for just three Portuguese estuarine systems: the Aveiro coastal Lagoon, the Douro and Sado estuaries[5]. The Douro, Tagus and Sado inner estuaries and their adjacent coastal waters behave as sources of CO_2 to the atmosphere[6], with fluxes ranging from 31 to 76 mol C m^{-2} d^{-1}, which corresponds to an additional source of 0.1% to the CO_2 emissions by the near-shore ecosystems[4]. However, the estuarine inorganic carbon dynamics has never been assessed.

This paper intends to partially fulfil this gap by focusing on the CO_2 dynamics along Tagus estuary (Fig. 1), Portugal, one of the largest western European estuaries in surface area. Spatial and temporal CO_2 variability is addressed in this estuary based on information obtained from 10 surveys carried out from 1999 to 2007. This

[1]Instituto Português do Mar e da Atmosfera (IPMA), I. P., Av. Brasília, 1449-006, Lisbon, Portugal. [2]Instituto Superior de Educação e Ciências de Lisboa (ISEC Lisboa), Lisbon, Portugal. [3]MARETEC, Instituto Superior Técnico, Universidade de Lisboa, Av. Rovisco Pais, 1049-001, Lisboa, Portugal. Correspondence and requests for materials should be addressed to A.P.O. (email: oliveira.ap.1@gmail.com)

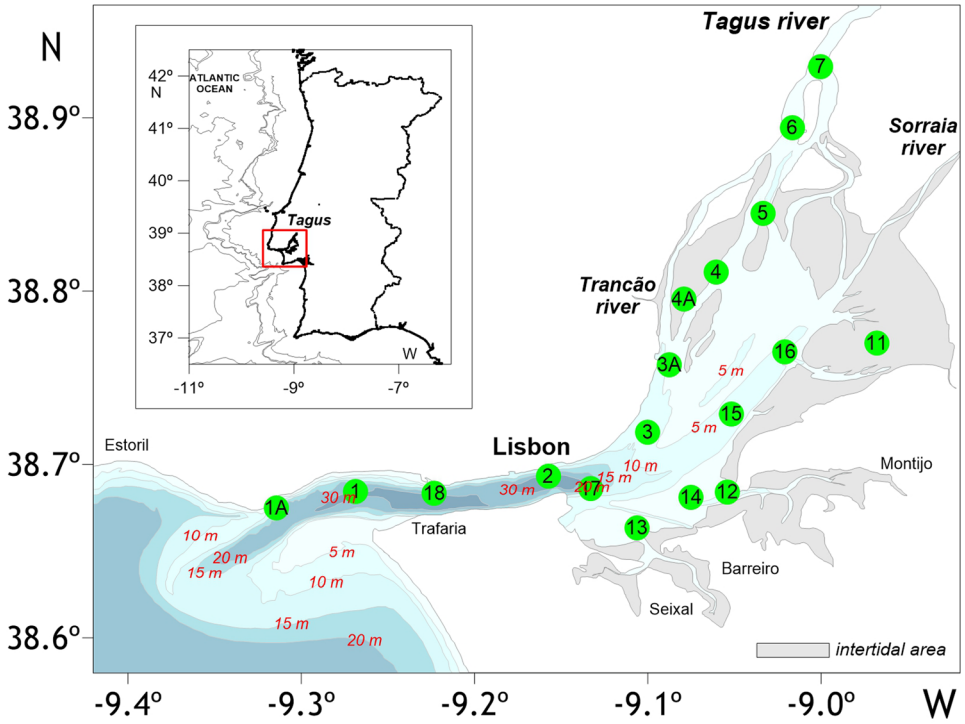

Figure 1. Map of Tagus estuary with the location of the sampling stations. Figure generated using the software Surfer Version 12.8.1009 (http://www.goldensoftware.com/products/surfer), a surface mapping system from Golden Software, LLC. Coastline and bathymetry were created based on Google "Map data: Google, Earth" (https://www.google.pt/maps/) and on data SIO, NOAA, U.S. Navy, NGA, GEBCO version 20141103 (http://www.gebco.net).

work also intends to identify and study the dominant factors/mechanisms influencing the inorganic carbon system. In addition, some estimates are advanced on the water-air CO_2 fluxes over the estuary.

Results

General water properties. The range of values for physical, chemical and biological variables from 1999 to 2007 is shown in Table 1. Overall, salinity increased downstream (Fig. 2A) with lower values in winter/autumn (Fig. 3A). The environmental conditions in the estuary end-members indicate that salinity kept reasonably stable at the marine influenced area in most samples (Table 1), the exception being winter seasons and May 2000. In March 2001 the river discharge peaked 1861 $m^3 s^{-1}$ and salinity did not exceed 12.5 in the estuary. A decrease in temperature from the upper to the lower estuary was observed during spring and summer (Fig. 2B). This was in contrast with winter and autumn, when an increase down the estuary was seen (Fig. 2C). While the amplitude of temperature was 12 °C in the river end-member, only 5 °C amplitude was recorded at the marine influenced area.

Due to hydrodynamic conditions imposed by the tidal regime (tidal amplitude of 1.5 to 4.0 m) and the water discharges (Tagus discharges from 33 to 1861 $m^3 s^{-1}$; Table 1), significant amounts of suspended matter spread all over the estuary (Fig. 2D). In general the amount of SPM in the estuary was low to moderate, rarely exceeding 80 $mg l^{-1}$ (Fig. 2D; Table 1).

Concerning oxygenation conditions, Tagus waters were always well oxygenated, in general displaying saturation levels above 70% (Table 1), with an increase from winter to spring/summer (Fig. 3B). Concentration of phytoplankton biomass (Chl *a*) reached a maximum of 73.4 $mg m^{-3}$ in May 2006, and hardly attained 3 $mg m^{-3}$ (Fig. 3C; Table 1) in the rest of the periods (winter/autumn). An increase of Chl *a* towards the fluvial section was generally observed.

Variations of inorganic carbon system parameters. pH values in the marine section were rather constant (amplitude 0.21; Fig. 4A), while the riverine end-member pH varied significantly (amplitude 1.10; Fig. 4A). Seasonally, pH showed scattered patterns and variations were not the same for all sampling periods (Fig. 5A): in autumn/winter more acidic features were noticed upstream (7.13–7.68) and increased downstream (7.83–8.03); in spring/summer, most of the time, more basic values were present upstream than downstream.

TA and DIC values were always lower in the riverine section than in the marine area, ranging between 977 µmol kg^{-1} in winter and 2587 µmol kg^{-1} in summer. These parameters displayed less irregular values in the marine influenced area and varied, respectively, from 1469 µmol kg^{-1} in winter to 2885 µmol kg^{-1} in summer (Fig. 4B,C). A negative correlation was found between riverine TA and average freshwater discharges ($r^2 = 0.482$, $p < 0.05$). TA and DIC increased from winter to spring/summer (Fig. 3E,F), with values varying from 1401 to

Season	Sampling dates	Q [a] ($m^3 s^{-1}$)	*S*	*T* (°C)	SPM ($mg l^{-1}$)	Chl *a* ($mg m^{-1}$)	DO (%)	pH	TA ($\mu mol kg^{-1}$)	DIC ($\mu mol kg^{-1}$)	pCO_2 (µatm)
Summer	September 1999[b]	33	4.66–36.00	14.1–22.0	16.4–39.6	1.5–14.4	79–106	7.23–7.91	2307–3381	2409–3323	922–4575
Spring	May 2000	376	0.17–26.96	17.8–20.8	6.1–71.3	1.0–13.5	82–103	7.82–7.88	1401–3535	1421–3455	906–1592
Winter	March 2001	1861	0.09–12.50	13.0–14.6	19.6–164.7	0.7–3.1	66–104	7.63–7.92	977–1834	1016–1816	873–1998
Summer	July 2001[b]	130	0.24–35.10	16.1–24.7	7.8–42.3	3.2–13.0	93–126	7.91–8.01	1918–2827	1954–2666	714–1326
Summer	June 2002[b]	81	0.31–34.27	17.7–24.3	28.6–135.0	1.4–40.1	87–104	7.70–8.23	2573–3330	2587–3270	1012–2779
Spring	May 2003[b]	233	0.20–34.12	16.6–23.4	5.7–62.0	1.6–31.8	85–107	7.54–7.94	1751–2784	1875–2672	851–3778
Winter	February 2004	264	0.18–23.51	12.7–15.7	11.5–64.5	0.2–2.6	78–91	7.13–8.05	1447–2792	1476–2639	662–9160
Spring	May 2006[b]	125	0.58–33.76	17.7–21.8	37.9–116.3	1.0–73.4	89–114	7.77–8.25	1418–3382	1422–3145	487–2704
Autumn	November 2006	768	0.21–32.39	17.7–19.0	32.3–56.8	0.2–1.1	72–90	7.35–7.90	1757–2884	1915–2717	1058–4552
Spring	May 2007[b]	86	9.81–35.23	14.8–20.9	12.0–45.0	1.4–9.4	82–101	7.89–8.05	2371–2528	2269–2366	620–970

Table 1. Range of physical-chemical and biological properties of surface waters in Tagus estuary for each sampling date. Freshwater flow (Q), salinity (*S*), temperature (*T*), suspended particulate matter (SPM), chlorophyll *a* (Chl *a*), dissolved oxygen (DO), total alkalinity (TA), dissolved inorganic carbon (DIC) and CO_2 partial pressure (pCO_2). [a]Tagus river flow, taken from Almourol station (the most downstream hydrological station, ~85 km upstream the estuary mouth). On-the-spot water discharge data was not available. Values were obtained from the Portuguese Environment Agency (APA, I.P.) accessed in a public database (http://snirh.apambiente.pt/) [b]Upwelling was present at the adjacent coastal shelf.

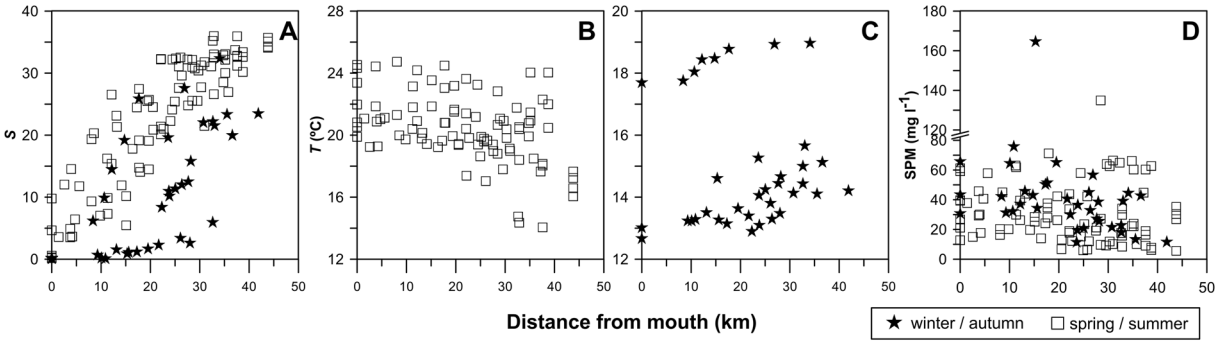

Figure 2. Longitudinal distributions of (**A**) salinity (*S*), (**B**) temperature (*T*) in spring/summer, (**C**) temperature (*T*) in winter/autumn and (**D**) suspended particulate matter (SPM), during the 10 surveys carried out along Tagus estuary. Riverine end-member: sampling station with lowest salinity; Marine end-member: sampling station nearest the ocean.

3535 µmol kg^{-1} during the productive period and from 977 to 2884 µmol kg^{-1} during the non-productive period (Table 1).

pCO_2 values were higher in the riverine section, reaching as high as 9160 µatm in February 2004 (Fig. 4D; Table 1), a value ~24 times higher than pCO_2 of atmospheric equilibrium (383.9 µatm). Seasonally average values of pCO_2 remain rather stabilized from winter to spring/summer and increased in autumn (Fig. 3G). Values of pCO_2 dropped rapidly in the upper estuarine zone (Fig. 5D) at salinities below 10. pCO_2 values as high as 9160 µatm (Table 1) were accompanied by low pH (7.13) at salinities below 5. Downstream, pCO_2 in general dropped to values of 620 µatm at the estuary mouth (Fig. 5D).

CO_2 evasion pattern. Table 2 shows CO_2 gas transfer velocities at the water-air interface, proposed by different authors and calculated for Tagus estuary, as well as wind speed and tidal current for each season. Daily wind velocity was random and variable, oscillating between 1.7 m s^{-1} and 3.9 m s^{-1}. The maximum tidal current was lower in summer (58 cm s^{-1}) and reached 122 cm s^{-1} in autumn depending on the tidal regime, river discharges and bathymetry of the estuary. Two of the algorithms used to estimate gas transfer velocity (*k*), namely k_{B04} [7] and k_{A09} [8], gave the highest values when compared with other algorithms. This was an expected outcome since both approaches are based on the same technique (floating dome) and took into account the water current velocity. The k_{OD58} [9] algorithm led to minimum *k* values, since it considers water current alone. However, maximum values of *k* were obtained in spring for all the parameterizations associated with maximum wind speed conditions (Table 2).

When applying a sensitive analysis to the fluxes calculated for each of the various parameterizations, differences emerged varying from 8 to 30%. Hence, in order to minimize any substantial errors in the fluxes estimated due to the use of a single generic relationship, CO_2 fluxes were averaged for the proposed parameterizations (k_{C96}, k_{RC01}, k_{B04} and k_{A09}). A seasonal pattern of CO_2 fluxes to the atmosphere was revealed in Tagus estuary, values increasing from 80.4 ± 87.7 mmol C m^{-2} d^{-1} in spring to 133.9 ± 89.3 mmol C m^{-2} d^{-1} in autumn (Table 2). Concerning spatial variability, the amplitude of fluxes variability was ~250 mmol C m^{-2} d^{-1} (calculated as the

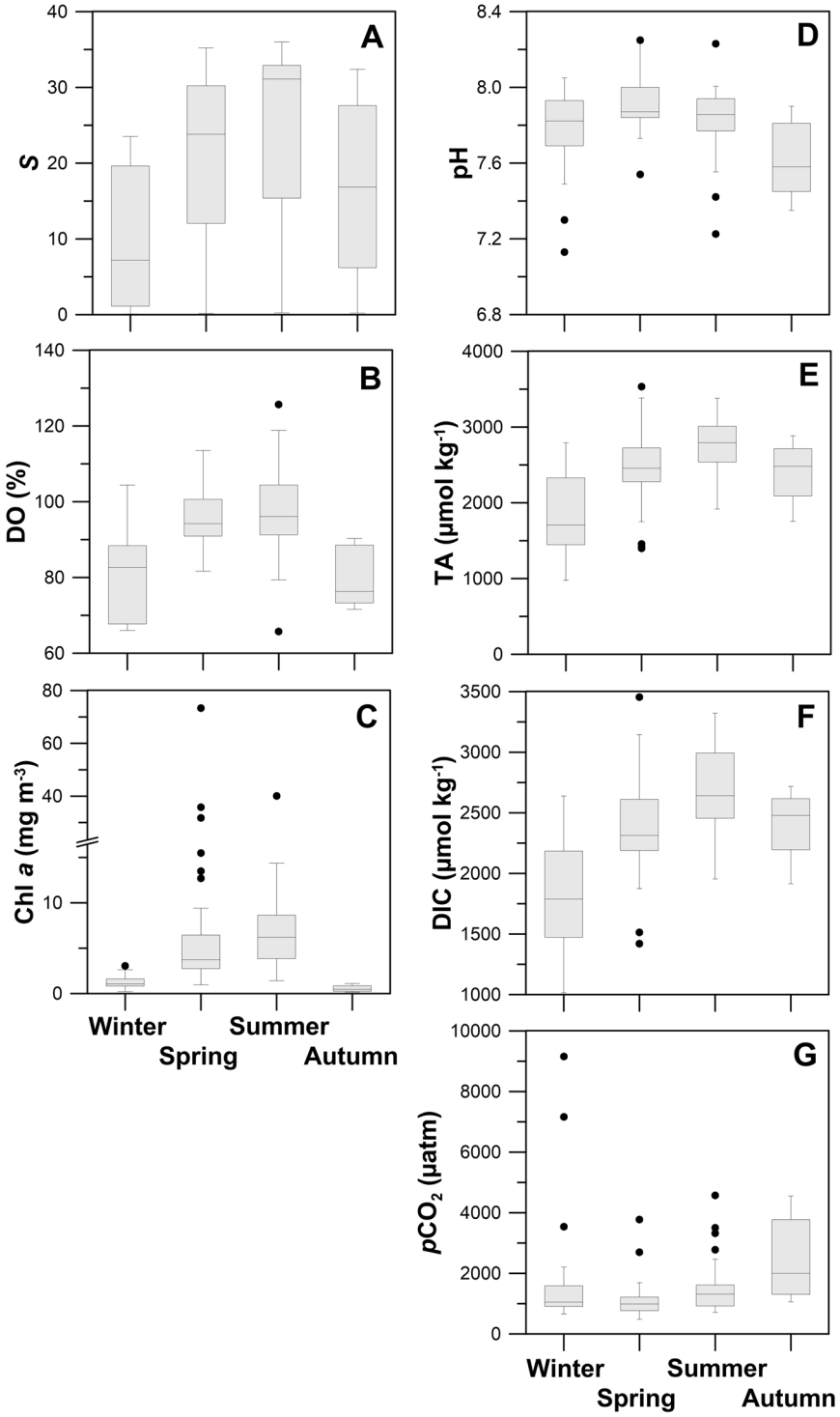

Figure 3. Box-whisker plot of (**A**) salinity (*S*), (**B**) dissolved oxygen (DO), (**C**) chlorophyll *a* (Chl *a*), (**D**) pH, (**E**) total alkalinity (TA), (**F**) dissolved inorganic carbon (DIC) and (**G**) CO_2 partial pressure (pCO_2) in Tagus estuary during 1999–2007. Median values are represented by line inside boxes, 25th to 75th percentiles are denoted by box edges, 10th to 90th percentiles are depicted by the error bars, and outliers are indicated by circles.

average of the difference between the least and greatest values observed for each sampling period) for the 10 surveys. Examples of CO_2 fluxes distribution along the estuary in different year seasons (March 2001, July 2001 and May 2006) are shown in Fig. 6.

Overall, Tagus estuary functions as a source of CO_2 to the atmosphere, being estimated an average annual flux of 33.6 ± 29.7 mol C m^{-2} yr^{-1} [6] and a total CO_2 emission of 0.11 Tg C yr^{-1}.

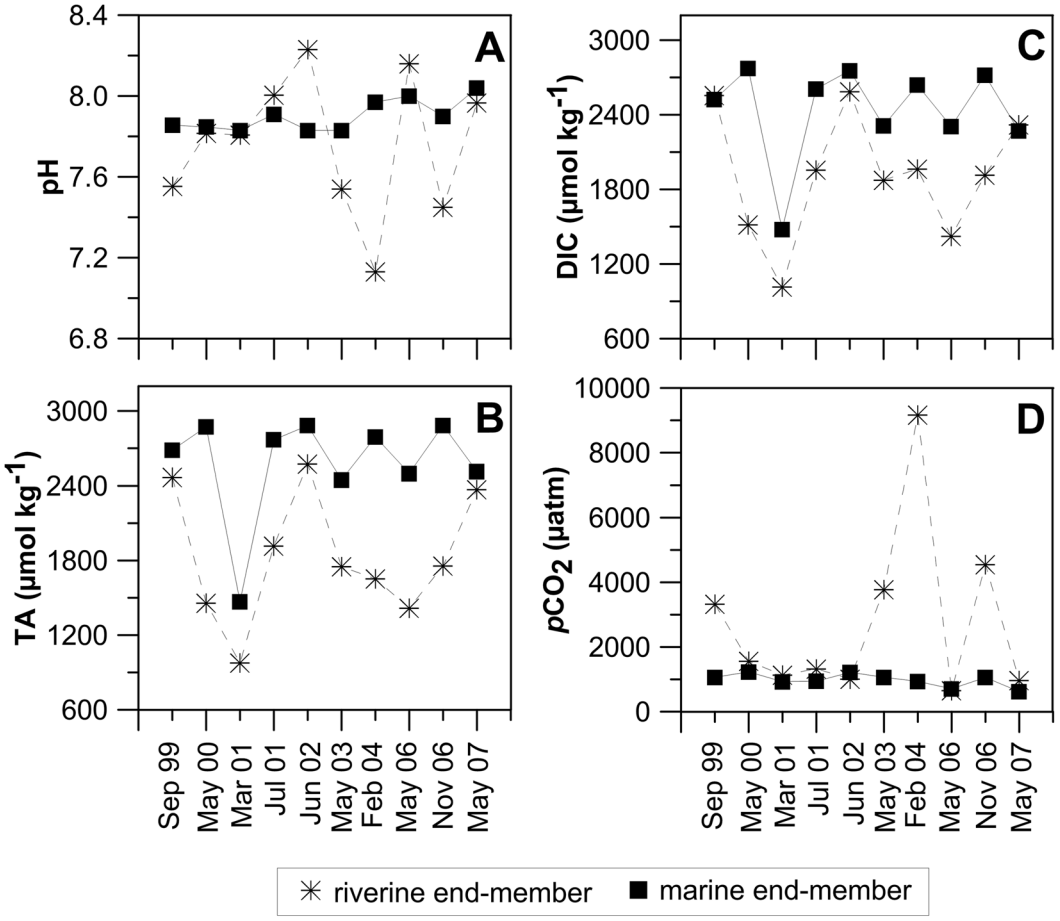

Figure 4. Riverine (✳) and marine (■) end-members values of (**A**) pH, (**B**) total alkalinity (TA), (**C**) dissolved inorganic carbon (DIC) and (**D**) CO_2 partial pressure (pCO_2) throughout to the 10 surveys undertaken in Tagus estuary.

Inorganic carbon balance. The following inorganic carbon fluxes were considered to establish the inorganic carbon balance in Tagus estuary: the riverine DIC input to the estuary, the estuarine DIC output to the adjacent coastal waters and the water-air CO_2 flux. Mixing curves of DIC for each sampling period (exception of September 1999 and May 2007) were well reproduced by polynomial equations (Table 3). DIC fluxes and advective export of DIC added during estuarine transport (Internal DIC Flux; Table 3) were estimated[10], and the magnitudes and temporal variation of inorganic carbon fluxes examined.

Freshwater end-member DIC concentration (C_0; Table 3) did not vary much during all survey periods (1786.9 ± 155.8 µmol kg^{-1}), except during an exceptionally intense river discharge in March 2001, and in June 2002, with low river flow and relatively high photosynthetic activity (Table 1). However, the estimates show that DIC riverine exports to the estuary varied from 16.6×10^6 mol C d^{-1} (summer 2001) to 179.2×10^6 mol C d^{-1} (winter 2001) (Table 3), with a mean annual flux of 0.27 Tg C yr^{-1}.

It was observed that during the estuarine transport, generated DIC ($C_S - C_0$) was higher in winter 2001 and lower (sometimes zero) in the other seasons. These internal fluxes ranged from 0 to 167.9×10^6 mol C d^{-1}, being estimated a mean annual internal flux of 0.10 Tg C yr^{-1} (Table 3). Fluxes from the estuary to the adjacent coastal waters varied from 16.6×10^6 mol C d^{-1} (in summer 2001) to 347.1×10^6 mol C d^{-1} (in winter 2001), corresponding to an annual flux of 0.37 Tg C yr^{-1} (Table 3). Thus, 27% of DIC was generated within the estuary, while the exported DIC to the atmosphere was 0.11 Tg C yr^{-1}, which accounted for approx. 23% of the total DIC exported from the estuary.

Discussion

Tagus waters environmental properties were strongly affected by the river discharge and showed a seasonal variability typical of a mid-latitude system, with most parameter values increasing from winter to spring/summer. Generally, river water carried higher contents of particulate material (Fig. 2D), nutrients (Fig. 7C) and phytoplankton (pers. comm.), than estuarine water. A tendency of a decrease ocean-ward was observed in winter, although high levels of SPM were present during the productive period in the 20–30 salinity range. This predominance of estuarine suspensions in the central/lower estuary can be interpreted as the result of salt marsh particles mixing and/or water circulation in the southern estuary, rather than the occurrence of biogeochemical processes.

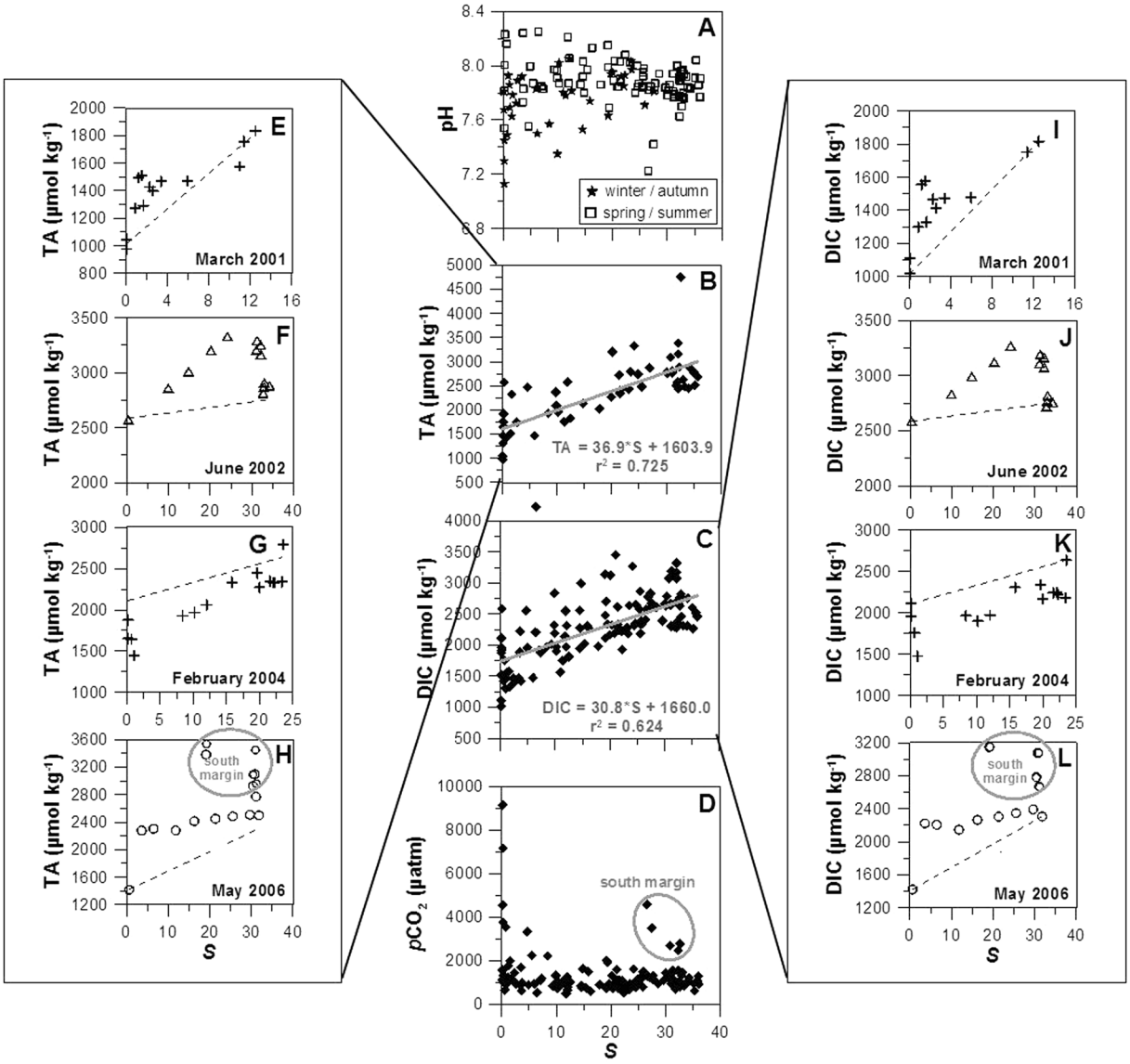

Figure 5. Mixing curves for (**A**) pH, (**B**) total alkalinity (TA), (**C**) dissolved inorganic carbon (DIC) and (**D**) CO_2 partial pressure (pCO_2) for all 10 surveys data undertaken in Tagus estuary. TA anomalies in (**E**) March 2001, (**F**) June 2002, (**G**) February 2004 and (**H**) May 2006. DIC anomalies in (**I**) March 2001, (**J**) June 2002, (**K**) February 2004 and (**L**) May 2006.

SPM values are comparable to values recorded for the Scheldt and the Thames estuaries and much lower (~14 times) than the ones in the highly turbid Gironde[11].

pH values in the marine section were rather constant due to the seawater buffering capacity, while the riverine end-member pH varied largely being such variability attributed to runoff coupled to changes in biological activity. pH seasonal trends can be attributed to more runoff in winter and more intense primary productivity, in particular in spring/summer, upstream. Overall, pH values were higher in spring/summer and lower in autumn/winter (Fig. 3D).

TA and DIC riverine values were similar to those reported for the uppermost sections of other estuaries[12–15]. To a certain extent, the seasonal variability of TA and DIC was related to the river discharge. Highest values occurred during the low flow period when higher salinity water dominates the estuary and the lowest during intense river discharges. TA and DIC plots against salinity (Fig. 5B,C) show values increasing downstream. These trends have also been recorded in other estuaries[13,14,16–19]. The nearly-conservative behaviour can be explained by the counterbalance between sources and consumption of TA and DIC along the salinity gradient. Nevertheless, non-conservative relationships were observed in March 2001 (Fig. 5E,I), June 2002 (Fig. 5F,J), February 2004 (Fig. 5G,K) and May 2006 (Fig. 5H,L).

Tagus estuary was dominated by supersaturated CO_2 conditions. Observed riverine pCO_2 values (up to 9160 µatm) are similar to other estuaries[3,17,19–23]. The upper Scheldt, for example, revealed values of pCO_2 as high as 9400 µatm[5] and as 15500 µatm[3]. Similar high values are reported for the Saja-Besaya estuary[22] (9728 µatm) at

	winter	spring	summer	autumn
Wind speed (m s^{-1})	3.7 ± 1.6	3.9 ± 1.8	3.3 ± 1.3	1.7 ± 0.7
Maximum tidal current speed (cm s^{-1})	103	80	58	122
ΔpCO_2 (µatm)	1337.1 ± 1930.8	674.2 ± 532.9	1147.4 ± 872.6	1908.6 ± 1277.8
k_{C96} (cm h^{-1})	5.0 ± 2.0	7.1 ± 3.7	4.9 ± 1.8	3.3 ± 1.4
k_{RC01} (cm h^{-1})	4.8 ± 1.7	8.1 ± 6.3	4.6 ± 1.3	3.3 ± 0.8
k_{B04} (cm h^{-1})	11.9 ± 3.6	14.9 ± 4.8	11.6 ± 2.7	9.9 ± 3.7
k_{A09} (cm h^{-1})	10.3 ± 3.6	14.1 ± 6.6	10.4 ± 3.2	7.3 ± 2.4
k_{OD58} (cm h^{-1})	4.6 ± 1.4	4.6 ± 1.5	4.0 ± 1.6	4.6 ± 2.9
Water current contribution (%)[a]	48	39	45	59
Water-air CO_2 flux (mmol C m^{-2} d^{-1})[b]	109.9 ± 83.9	80.4 ± 87.7	86.9 ± 64.6	133.9 ± 89.3
CO_2 emission (10^6 mol C d^{-1})[c]	29.0	21.2	23.0	35.3

Table 2. Tagus estuary seasonal values for daily average wind speed, maximum tidal current speed, pCO_2 gradient (ΔpCO_2), CO_2 gas transfer velocity (k) given by the parameterizations of Carini *et al.*[42] (k_{C96}), Raymond and Cole[43] (k_{RC01}), Abril *et al.*[8] (k_{RC01}), Borges *et al.*[7] (k_{B04}) and O'Connor and Dobbins[9] (k_{OD58}), water current contribution, water-air CO_2 fluxes and CO_2 emission. [a]calculated as the ratio $k_{OD58}/(k_{OD58} + k_{C96})$ [b]averaged CO_2 water-air fluxes for the four parameterizations proposed (k_{C96}, k_{RC01}, k_{B04} and k_{A09}) [c]surface area of 265 km^2 computed as the definite integral of bidimensional masks defined from latitude, longitude, and coastline information, using the ferret software.

salinities below 5, and a range of 1000 to >6000 µatm at low-salinity areas in the Satilla and Altamaha Rivers[17]. As suggested by some authors[19,21,23–25], high pCO_2 values at riverine waters might be due to organic carbon mineralization in soils, river waters and sediments. Differences in inorganic carbon variability patterns in the two end-members indicate, beside the dilution effect, the complexity of interactions between input sources and processes acting along the estuary. Spatial trends and range of values for this estuary are also similar to those reported for other estuaries[4,5,14,18,19].

Mixing curves are a commonly used approach for the interpretation of source/sink dynamics of estuarine constituents[10,13,26]. Assuming salinity as a satisfactory mixing indicator, the profiles of water properties as functions of salinity should be linear, if only mixing processes occur in an estuary. Thus, analysis of correlations between different parameters was used for identification of other processes in Tagus estuary.

As mentioned above, CO_2 parameters behaved conservatively in most of the sampling periods, with the system dominated by mixing processes. But comparing the TA/DIC salinity profiles with theoretical mixing lines drawn between the two end-members, TA/DIC anomalies came out in the upper estuary at salinities below 10. In June 2002 an anomaly occurred at higher salinities in the middle estuary. Positive anomalies in TA/DIC mixing curves (TA/DIC concentrations lie above the theoretical mixing line) occurred in March 2001, as well in June 2002 and May 2006, and a negative anomaly occurred in February 2004. Thus, the non-linearity of TA and DIC distributions indicates that other processes are responsible for the inorganic carbon variability in some occasions. Actually, a non-conservative behaviour of TA and DIC in upper estuaries, mostly at salinities below 5, has been referred by some authors[27].

In March 2001, an exceptional river discharge (1861 m^3 s^{-1}; Table 1) occurred, probably not allowing enough time for biogeochemical reactions to occur in the estuary[28]. However, a mechanism involving increase of pCO_2 and decrease of pH and DO (Fig. 7A) has been hypothesized to be the aerobic respiration. Such mechanism would lead, nevertheless, to DIC increase and would have practically no effect on TA. Still, the simultaneous increase in both parameters (TA and DIC) was observed, pointing to a distinct process responsible for TA production, possibly calcium carbonate ($CaCO_3$) dissolution. To assess this possibility, $CaCO_3$ saturation state was calculated for calcite and aragonite (respectively Ω_c and Ω_a), using the thermodynamic solubility products[29]. Calculations have shown that for this high flow period, the estuary was undersaturated with values of Ω_c and Ω_a varying from 0.01 to 1.02, eventually indicating $CaCO_3$ dissolution. This process has referred to as the generator of alkalinity in Loire and Godavari estuaries[27,30].

In June 2002, a TA/DIC deviation from linearity was noticed in the central part of the estuary, at salinities approximately 20–30 (Fig. 5F,J). A production of TA of ca. 540 and of ca. 565 µmol kg^{-1} of DIC was estimated by comparing the theoretical mixing line to *in situ* values. The anthropogenic influence of Trancão River (Fig. 1) in that zone, with high loads of organic carbon and associated mineralization, may explain such increase in TA. Additionally, the concomitant decrease of pH and DO and increases of pCO_2 (Fig. 7C), as well as of SPM and nitrate, decrease at that respective range of salinities (Fig. 7B), supports the occurrence of organic carbon mineralization. The considerable amount of suspended matter attained in that region (Fig. 7C) may have favoured some carbonate dissolution as well. In fact, it has been reported the occurrence of dissolution of $CaCO_3$ and consequent generation of alkalinity in other estuaries, in zones of maximum turbidity, namely in Loire[27] and in the highly turbid Gironde[31] and Ems[32].

A strong decrease of TA/DIC (430 and 640 µmol kg^{-1}, respectively for TA and DIC) was observed during February 2004 (Fig. 5G,K) in the extremely low range of salinity (from 0 to 1), accompanied by a relatively conservative ($r^2 = 0.765$, $p < 0.05$, $n = 12$) behaviour downstream. Simultaneously, pCO_2 attained extremely high values (9160 µatm), contrasting with the values obtained in other sampling surveys (hardly attaining 4500 µatm; Table 1). This might be explained by the efflux of CO_2 to the atmosphere in the very low salinities region, leading

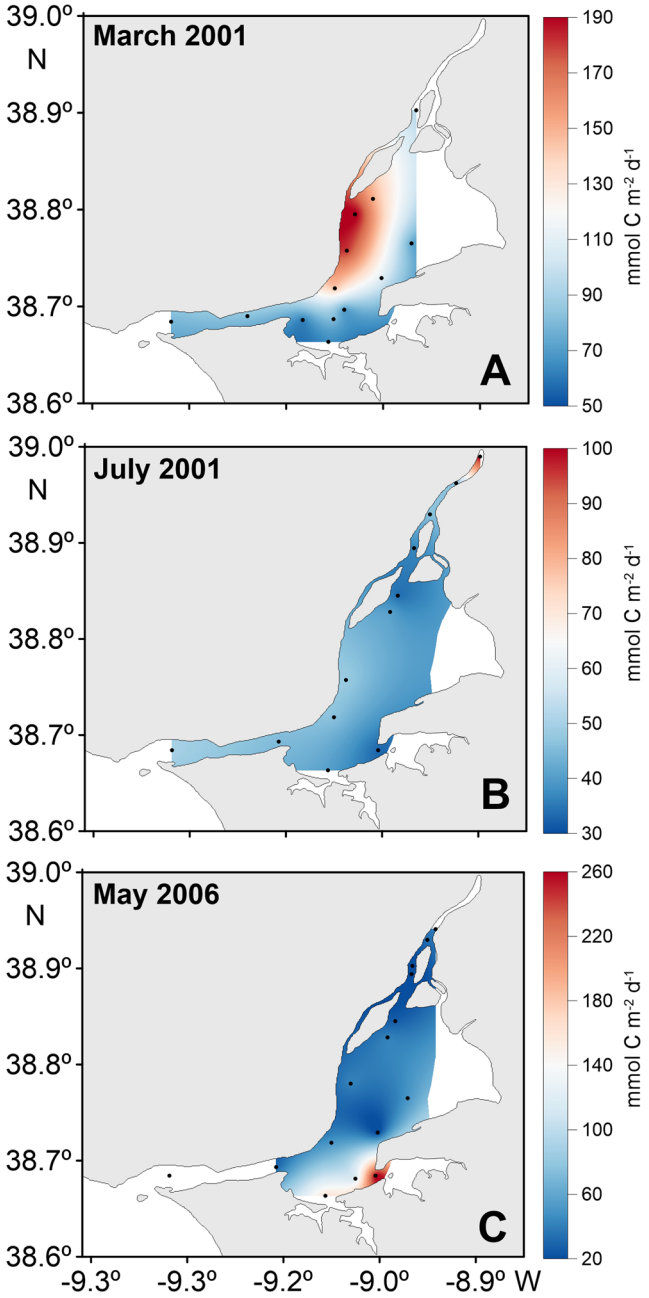

Figure 6. Water-air CO_2 fluxes (mmol C m^{-2} d^{-1}) distribution along Tagus estuary in (**A**) March 2001, (**B**) July 2001 and (**C**) May 2006. Figure generated using the software Surfer Version 12.8.1009 (http://www.goldensoftware.com/products/surfer), a surface mapping system from Golden Software, LLC. Coastline and bathymetry were created based on Google "Map data: Google, Earth" (https://www.google.pt/maps/) and on data SIO, NOAA, U.S. Navy, NGA, GEBCO version 20141103 (http://www.gebco.net).

to the consumption of TA/DIC. Moreover, Chl *a* values (just up to 2.6 mg m^{-3}; Table 1) reflecting winter conditions, support the above conclusion, since photosynthetic carbon fixation very unlikely would justify TA/DIC consumption. At salinity 20 another decrease of TA/DIC (~270 µmol kg^{-1}) occurred, which also might correspond to CO_2 degassing reflected in the decrease of pCO_2 from 920 µatm to 670 µatm.

In May 2006, TA/DIC increase at low salinities seemed to be due to a combination of processes. Even if considerable primary productivity was underway in that region, reflected in elevated Chl *a* values (up to 73.4 mg m^{-3}; Table 1), low pCO_2 (487–650 µatm) and as well as relatively high pH (8.25; Table 1), consumption of TA/DIC did not occur, as expected for high phytoplankton biomass development. As no clear evidence of particulate organic matter mineralization was revealed, a possible explanation for production of DIC in that range of salinity could be mineralization of labile organic material (mainly glicids) produced by phytoplankton exudation and/or lysis. Thus, it means that photosynthetic activity might indirectly contribute to DIC increase, counteracting the

Season	Sampling dates	DIC (μmol kg^{-1}) as a function of S	r^2	C_0[a] (μmol kg^{-1})	C_S[b] (μmol kg^{-1})	Freshwater DIC Flux (10^6 mol C d^{-1})	Internal DIC Flux (10^6 mol C d^{-1})	Estuarine DIC Flux (10^6 mol C d^{-1})
Spring	May 2000	43.1 S + 1540.7	0.774	1540.7	1540.7	51.0	0	51.0
Winter	March 2001	$-29.2\ S^2 + 230.0$ S + 1110.5	0.628	1110.5	2151.2	179.2	167.9	347.1
Summer	July 2001	23.5 · S + 1815.0	0.903	1815.0	1815.0	16.6	0	16.6
Summer	June 2002	$-1.5\ S^2 + 63.4$ S + 2481.5	0.527	2481.5	4243.2	17.8	12.6	30.5
Spring	May 2003	14.4 S + 1818.4	0.948	1818.4	1818.4	37.6	0	37.6
Winter	February 2004	$0.7\ S^2 + 6.7 \cdot S + 1832.7$	0.602	1832.7	1445.8	42.5	−9.0	33.5
Spring	May 2006	$-1.3 \cdot S^2 + 59.6$ S + 1704.1	0.629	1704.1	3018.7	18.9	14.6	33.5
Autumn	November 2006	21.2 S + 2010.5	0.739	2010.5	2010.5	136.4	0	136.4
Annual mean values (Tg C yr^{-1})						0.27	0.10	0.37

Table 3. Dissolved Inorganic Carbon (DIC) distributions and fluxes in Tagus estuary. Equations are polynomial equations used to fit the data from DIC *versus* salinity for each sampling transects. All equations have $p < 0.05$. C_0 and C_S are, respectively, freshwater and seawater DIC concentrations. The flux of freshwater DIC is defined as $(Q \cdot C_0)$, whereas the flux of internal DIC is $(Q \cdot (C_S - C_0))$ and the estuarine flux is $(Q \cdot C_S)$. Q represents the Tagus River flow. [a]DIC concentration where the polynomial equation intersects the y-intercept (or the concentration at zero salinity) [b]DIC concentration where the tangent at the marine end-member crosses the y-intercept

expected decrease under conditions of relatively high productivity. Besides, another mechanism likely acting and leading to generation of alkalinity may have been dissolution of $CaCO_3$, as by this period only slightly supersaturated conditions were present in the estuary.

It should be taken into account that the patterns of TA and DIC could also be related to other processes. As about one third of Tagus estuary surface is composed by intertidal areas, sediments are sites of organic matter degradation[33]. Moreover, salt marshes sediments store carbon and their pore waters enriched in DIC are transferred to the estuary waters by tidal pumping, also producing DIC. This mechanism has been reported to act in mangrove creek[34,35] as well. In addition, denitrification occurs in Tagus[36], and it is known that such processes were responsible for TA increases in several estuaries[17,31,34,37].

The predominance of CO_2 supersaturation conditions in Tagus estuary suggests that the system is dominated by heterotrophy[6], which is backed by the O_2 data (pers. comm.). The highest pCO_2 values were noticed at the salinity ranges 0–5 and also 20–30 (Fig. 5D). Upstream pCO_2 was most likely originated from riverine waters probably having no time to degas. pCO_2 increase observed at higher salinities might be attributed to lateral transport of CO_2 from salt marshes mainly located at the southern margin of Tagus in the north margin near the polluted Trancão River.

Studies carried out in Tagus marshes in 2001/2002 revealed CO_2 supersaturation, and pCO_2 values varying from 877 to 3950 μatm (Oliveira, unpublished data). Besides, other studies suggest that in tidally flooded salt marshes of some estuaries of Georgia/U.S.A, the CO_2 supersaturation was controlled by inputs from organic carbon respiration[17,38]. Also, CO_2 supersaturation of three Georgia estuaries were due to CO_2 inputs from the intertidal marshes and the rivers[39]. Thus, within Tagus estuary, mechanisms such as mixing of supersaturated freshwater with seawater, CO_2 efflux to the atmosphere and carbonate dissolution seem to emerge as the major regulators of pCO_2 spatial distribution.

As mentioned in another study[6], higher CO_2 emissions were generally related to more intense wind speed, although no statistical significance was observed ($p > 0.05$). Tagus estuary water current was found to largely affect the gas transfer velocity over it (~48% on average) (Table 2), an effect estimated by applying the ratio $k_{OD58}/(k_{OD58} + k_{C96})$.

The value is rather high when compared with estimates for other European estuaries, such as the Scheldt (25%)[40] and Guadalquivir (30%)[41]. Assuming that water current and wind speed have an additive effect on k[7], the water current expression proposed by O'Connor and Dobbins[9] was combined with the algorithms from Carini *et al.*[42] and Raymond and Cole[43]. The outcome of the respective additive effect resulted in $k'_{C96} = k_{C96} + k_{OD58}$ and $k'_{RC01} = k_{RC01} + k_{OD58}$. Also, the possibility of a fetch effect on k has been investigated. Since the suspended matter levels present in the estuary were low to moderate (<165 mg l^{-1}; Table 1) it was assumed that turbidity might have a rather limited effect on k.

Tagus estuary was always CO_2 supersaturated inducing effluxes to the atmosphere at an average flux of 33.6 ± 29.7 mol C m^{-2} yr^{-1} leading to an average CO_2 emission of 0.11 Tg C yr^{-1}. Tagus CO_2 fluxes are similar to the ones estimated for some inner estuaries (32.1 mol C m^{-2} yr^{-1}) and analogous to fluxes of other European estuaries like Sado/Portugal (31.1 mol C m^{-2} yr^{-1}), Gironde/France (30.8 mol C m^{-2} yr^{-1}) and Guadalquivir/Spain (31.3 mol C m^{-2} yr^{-1})[4,6].

The nearly-conservative DIC distribution observed most of the time along the estuary implies that inputs and outputs are in equilibrium, meaning that the CO_2 flux to the atmosphere must be balanced by net CO_2 production in the water column or sediment. In fact, several researchers[13,20,38,44] referred the dynamic coupling between CO_2 generation and evasion being extremely fast in estuaries.

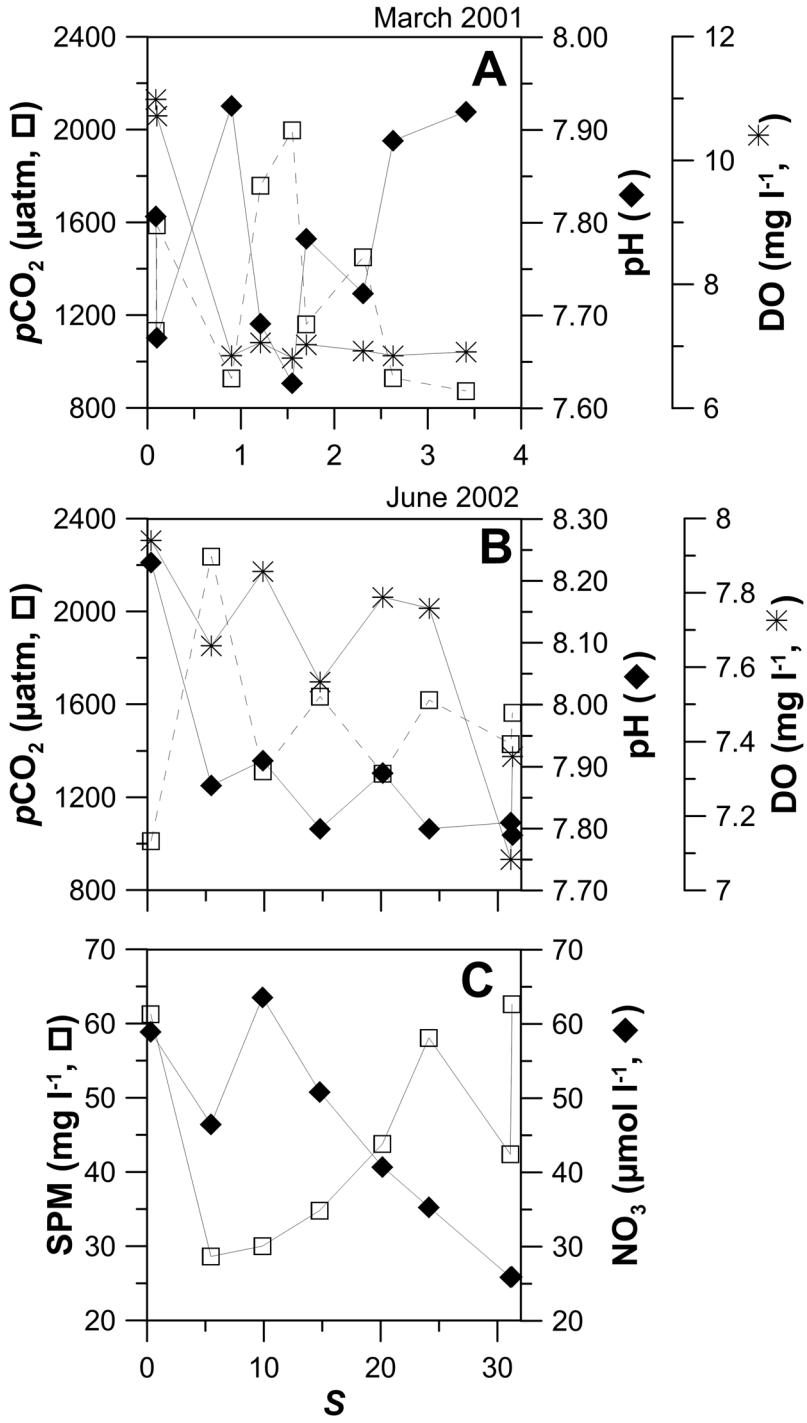

Figure 7. Distributions of CO_2 partial pressure (pCO_2), pH and dissolved oxygen (DO) along the salinity gradient in (**A**) March 2001 and in (**B**) June 2002. Also, distributions of (**C**) suspended particulate matter (SPM) and nitrate (NO_3) in June 2002 along the salinity gradient in Tagus estuary.

Freshwater end-member DIC concentration did not vary much during all survey periods. Such near stable values suggest that the concentration of the inorganic carbon entering the estuary is, to a certain extent, independent of the season of the year and very likely independent of the Tagus discharges.

The relative contribution of riverine CO_2 to the overall CO_2 emission by the estuary (estimated after[45]) was ~6% in spring and ~10% in autumn. In fact, these values are very close to those reported for the very productive Scheldt estuary (10%)[45] and for 11 European estuaries (median value 10%)[46]. Still, that proportion can be highly variable from one estuary to the other, for example for the Randers Fjord the riverine contribution reached a value of 50%[46], for Guadalquivir estuary 30%[41] and for Rhine estuary ~300%[46]. Hence, most of the emission of CO_2 from Tagus estuary (~90%) was attributed to heterotrophic activity.

Our study suggests that changes in the Tagus estuary carbonate parameters seemed to be consequence of rather more complex feature than just the result of simple mixing of freshwater and seawater. Riverine/terrestrial runoff and occurrence of specific biogeochemical processes as photosynthesis, aerobic respiration, organic matter mineralization (degradation) and $CaCO_3$ precipitation/dissolution might be responsible for carbonate variability. Probably, the pore waters rich in DIC transferred to the estuary waters by tidal pumping may also contribute to the occurred changes. The inorganic carbon budget revealed that 0.27 Tg C enter into Tagus estuary annually, while 0.37 Tg C are exported to the adjacent coastal waters. Overall, 23% of the total DIC exported from Tagus estuary is emitted to the atmosphere, and about 8% of riverine DIC is ventilated. Most of the estuarine emissions (average flux of 33.6 ± 29.7 mol C C m^{-2} yr^{-1}) were attributed to heterotrophy.

Methods

Geographic coverage. Tagus Estuary (Fig. 1) is located at the southwest Portugal (38°36′–39°N, 08°54′–09°24′W) and supports important human communities and natural resources. It is an inundated valley with a submerged area of 320 km^2 where ~40% are intertidal areas (~20 km^2 salt marsh vegetation and ~80 km^2 mudflats). This mesotidal estuary (tidal range 1–4 m) has a narrow and fault-controlled inlet channel separating two distinct regions: an outer wave-dominated area from an inner broad and tide-dominated part. Winds predominate from south and southwest during winter, rotating progressively to the northwest and north directions during spring, and maintaining these directions throughout the summer months. There is a strong seasonal hydrodynamic and biogeochemical variability due to seasonal fluctuations in meteorological conditions and river discharges (mean annual flow of 350 m^3 s^{-1}). There is also a strong horizontal gradient inside the estuary as a result of the hydrodynamic conditions, mostly tidally-controlled, with a dominant semidiurnal period and maximum amplitude of 4.8 m in spring tide. Middle estuarine areas, and to a lesser extent upper areas, have more stable and homogenous conditions, displaying a higher residence time. Lower estuarine areas, influenced by the tidal regime, are characterized by high variability. The mean residence time of water in the estuary varies between 26 and 8 days[47]. The system is vertically well-mixed and has a mean tidal prism of 600×10^6 m^3, about a third of the mean volume.

Even with recent reduction in organic loadings due to the implementation of considerable sewage treatment plants, the Tagus estuary is under intense anthropogenic disturbance, with a major population centre within its catchment basin (~2.3 million of inhabitants).

Sampling, analysis and calculation methods. The sampling period was from 1999 to 2007, covering an area extending from the estuary mouth to the point where freshwater was encountered. Sampling locations were selected to provide a full coverage of the salinity gradient (from 0 to 35). Surface seawater samples were collected at ebb conditions with Niskin bottles, for a total of 18 sites along a ~50 km stretch of the estuary (Fig. 1). Temperature (*T*) and salinity (*S*) parameters were determined *in situ* with a CTD (Conductivity - Temperature - Depth) Aanderaa probe. Salinity was calibrated with an AutoSal salinometer using IAPSO standard seawater, with a variation coefficient of 0.003%.

Dissolved oxygen (DO) was analysed following the Winkler method[48] using a whole-bottle manual titration. The coefficient of variation associated with the method ranged from 0.08 to 0.25%. pH was measured immediately after sample collection at 25 °C, using a Metrohm 704 pH-meter and a combination electrode (Metrohm) standardised against 2-amino-2-hydroxymethyl-1,3-propanediol seawater buffer (ionic strength of 0.7 M), at a precision of 0.005 pH units[49]. Total alkalinity (TA) samples were filtered through Whatman GF/F (0.7 μm) filters, fixed with $HgCl_2$ and stored (refrigerated not frozen) until use. Samples were then titrated automatically with HCl (~0.25 M HCl in a solution of 0.45 M NaCl) past the endpoint of 4.5[49], with an accuracy of ± 2 μmol kg^{-1}. The respectively accuracy was controlled against certified reference material supplied by A.G. Dickson (Scripps Institution of Oceanography, San Diego, USA).

Chlorophyll *a* (Chl *a*) was determined by filtering triplicate aliquots of ~150 ml water through Whatman GF/F filters (0.7 μm) under a 0.2 atm vacuum, and immediately frozen and later extracted in 90% acetone for analysis in a fluorometer Hitachi F-7000, calibrated with commercial solutions of Chl *a* (Sigma Chemical Co.). The variation coefficient was 1.8%. For suspended particulate matter (SPM) determinations, six aliquots of 100–1000 ml water samples were filtered through pre-combusted (2 h at 450 °C) Wathman GF/F filters and determined gravimetrically (drying at 70 °C). The respective filters were subsequently used for particulate organic (POC) and inorganic (PIC) carbon determinations using a CHN Fissons NA 1500 Analyser, with acetanilide as the calibration standard. System blanks were obtained by running several empty ashed tin capsules. The analyser provides a measure of total carbon, so the inorganic fraction was removed by drying the filters at 450 °C. The method precision was of 0.47%.

Meteorological data. Wind speed and direction were measured *in situ* with a Vaisala® meteorological station (Datalogger Campbell Scientific CR510) coupled with a MetOne 034 A anemometer. Continuous measurements were acquired with 1-minute intervals at 11 m height. Wind speed was referenced to a height of 10 m (u_{10})[50]. We assume one standard deviation of ± 2 m s^{-1} as wind speed error. Atmospheric CO_2 data was obtained from the Terceira Island's reference station (Azores, Portugal, 38.77°N 27.38°W), from the network of the National Oceanic and Atmospheric Administration (NOAA)/Climate Monitoring and Diagnostics Laboratory (CMDL)/Carbon Cycle Greenhouse Gases Group (CCGG)[51]. Some algorithms[49] were used to convert observed atmospheric CO_2 content in mole fraction (in dry air) to wet air values. Direct measurements of atmospheric CO_2 partial pressure made on-board was only available for some sampling periods. Significant correlations were found out between Terceira data and shipboard data ($r^2 = 0.910$, $p < 0.05$, $n = 45$) and the discrepancies lied just between 3 and 13 μatm. The impact of using Terceira data on this study was considered negligible.

Estimated parameters. pH values corrected to *in situ* temperature were calculated from total alkalinity (TA) and *in situ* pH and temperature[52]. For these calculations the carbon dioxide constants of Millero *et al.*[53] were applied.

The partial pressure of CO_2 in seawater (pCO_2) and the dissolved inorganic carbon (DIC) were calculated from the *in situ* temperature, TA and corrected pH, using the carbonic acid dissociation constants given by Millero *et al.*[53] and the CO_2 solubility coefficient of Weiss[54]. Errors associated with pCO_2 and DIC calculations were estimated to be ± 10 μatm and ± 5 μmol kg^{-1}, respectively (accumulated errors on TA and pH).

The water-air CO_2 fluxes (CO_2 Flux) were computed according to:

$$CO_2\,\text{Flux} = k \cdot K_0 \cdot \triangle pCO_2 \quad (1)$$

where k is the CO_2 gas transfer velocity, K_0 the solubility coefficient of CO_2 and ΔpCO_2 the water-air gradient of pCO_2. Positive CO_2 flux indicates emission of CO_2 from water to the atmosphere and negative flux the opposite direction.

Some authors[7,55,56] suggest that k–wind speed relationships are site-specific. More recently, it was argued[8] that wind, water current, surface area and turbidity, all significantly affect k in estuaries. Various measurement techniques on the gas transfer velocity in estuaries have been implemented, using methods such as dual tracer addition[42], natural gas tracer[57] or floating dome technique[7]. The tracer methods involve long term measurement of k over the entire estuary, while the floating dome technique is a short term measurement affected by the system heterogeneity that is typical in estuaries. In any case, the selection of a particular value for k will affect the overall representation of the net ecosystem metabolism. Since k was not determined *in situ* in Tagus estuary, we based our calculations to bracket the most likely value for k on parameterizations used on similar studies: (1) from a SF6 release experiment in the Parker River and estuary[42] (hereafter referred to as C96), (2) from a compilation of published k values in various rivers and estuaries, using different methodologies[43] (hereafter referred to as RC01), (3) considering the contribution of the water current[7,9] (hereafter referred to as B04), and (4) based on a generic equation that gives k as a function of water current velocity, wind speed, estuarine surface area and suspended matter content[8] (hereafter referred to as A09). The choice of these formulations was motivated by the relative similarity between the Tagus estuary and the systems studied by the mentioned studies, in their physical characteristics (e.g., shallow, well-mixed, influenced by tides). Water current and tidal height data at Tagus estuary were obtained with hindcast simulations using the MOHID Modelling System (www.mohid.com), based on real forcing for river discharge, tide and wind[58–60].

Estimated DIC fluxes. The internal flux of dissolved constituent was estimated based on mixing curves[10], by quantifying how much DIC was added by net heterotrophy during estuarine transport through DIC *versus* salinity plots. Whenever the distribution of a dissolved constituent is continuous and predictable using simple polynomial equations, C_0 is where the polynomial equation defining DIC concentrations intersects the y-intercept (or the concentration at zero salinity), and C_S is the concentration of the constituent where the tangent at the seawater end-member crosses the y-intercept. Still, total exported flux from the estuary is given by $(Q \cdot C_S)$, where Q is the freshwater flow, $(Q \cdot (C_S - C_0))$ the internal flux, and $(Q \cdot C_0)$ the flux from the freshwater end-member.

Statistical analysis. Exploratory analysis and statistical procedures were implemented using the statistical software Statistica 6.0® (Statsoft Inc., 2001). Differences between sampling periods in the measured/calculated physical-chemical and biological parameters, were assessed using an analysis of variance (ANOVA), and differences between means have been considered statistically significant for $p < 0.05$. The dominant processes influencing surface water chemistry were identified using linear correlations between the system parameters.

References

1. Gattuso, J. P., Frankignoulle, M. & Wollast, R. Carbon and carbonate metabolism in coastal aquatic ecosystems. *Annu. Rev. Ecol. Syst.* **29** (1998).
2. Chen, C. T. A. *et al.* Air-sea exchanges of CO2 in the world's coastal seas. *Biogeosciences* **10**, 6509–6544, doi:10.5194/bg-10-6509-2013 (2013).
3. Hellings, L., Dehairs, F., Van Damme, S. & Baeyens, W. Dissolved inorganic carbon in a highly polluted estuary (the Scheldt). *Limnol. Oceanogr.* **46**, 1406–1414 (2001).
4. Chen, C.-T. A. & Borges, A. V. Reconciling opposing views on carbon cycling in the coastal ocean: continental shelves as sinks and nearshore ecosystems as sources of atmospheric CO_2. Deep Sea Res. Pt II 56, 10.1016/j.dsr2.2009.01.001 (2009).
5. Frankignoulle, M. *et al.* Carbon dioxide emission from European estuaries. *Science* **282**, 434–436, doi:10.1126/science.282.5388.434 (1998).
6. Oliveira, A. P., Cabeçadas, G. & Pilar-Fonseca, T. Iberia coastal ocean in the CO_2 sink/source context: Portugal case study. *J. Coast. Res.* **28**, 184–195, doi:10.2112/jcoastres-d-10-00060.1 (2012).
7. Borges, A. V. *et al.* Gas transfer velocities of CO_2 in three European estuaries (Randers Fjord, Scheldt, and Thames). *Limnol. Oceanogr.* **49**, 1630–1641 (2004).
8. Abril, G., Commarieu, M. V., Sottolichio, A., Bretel, P. & Guerin, F. Turbidity limits gas exchange in a large macrotidal estuary. *Estuar. Coast. Shelf S.* **83**, 342–348, doi:10.1016/j.ecss.2009.03.006 (2009).
9. O'Connor, D. J. & Dobbins, W. E. Mechanism of reaeration in natural streams. *Trans. American Soc. Civil Eng.* **123**, 641–684 (1958).
10. Kaul, L. W. & Froelich, P. N. Modeling Estuarine Nutrient Geochemistry in a Simple System. *Geochim. Cosmochim. Ac.* **48**, 1417–1433, doi:10.1016/0016-7037(84)90399-5 (1984).
11. Abril, G. *et al.* Behaviour of organic carbon in nine contrasting European estuaries. *Estuar. Coast. Shelf S.* **54**, 241–262, doi:10.1006/ecss.2001.0844 (2002).
12. Cai, W. J. *et al.* The biogeochemistry of inorganic carbon and nutrients in the Pearl River estuary and the adjacent Northern South China Sea. *Cont. Shelf Res.* **24**, 1301–1319, doi:10.1016/j.csr.2004.04.005 (2004).
13. Raymond, P. A., Bauer, J. E. & Cole, J. J. Atmospheric CO2 evasion, dissolved inorganic carbon production, and net heterotrophy in the York River estuary. *Limnol. Oceanogr.* **45**, 1707–1717 (2000).

14. Brasse, S., Nellen, M., Seifert, R. & Michaelis, W. The carbon dioxide system in the Elbe estuary. *Biogeochemistry* **59**, 25–40, doi:10.1023/a:1015591717351 (2002).
15. Wang, Z. A., Cai, W. J., Wang, Y. C. & Ji, H. W. The southeastern continental shelf of the United States as an atmospheric CO2 source and an exporter of inorganic carbon to the ocean. *Cont. Shelf Res.* **25**, 1917–1941, doi:10.1016/j.csr.2005.04.004 (2005).
16. Devol, A. H., Quay, P. D., Richey, J. E. & Martinelli, L. A. The Role of Gas-Exchange in the Inorganic Carbon, Oxygen, and Rn-222 Budgets of the Amazon River. *Limnol. Oceanogr.* **32**, 235–248 (1987).
17. Cai, W. J. & Wang, Y. The chemistry, fluxes, and sources of carbon dioxide in the estuarine waters of the Satilla and Altamaha Rivers, Georgia. *Limnol. Oceanogr.* **43**, 657–668 (1998).
18. Guo, X. H. *et al*. Seasonal variations in the inorganic carbon system in the Pearl River (Zhujiang) estuary. *Cont. Shelf Res.* **28**, 1424–1434, doi:10.1016/j.csr.2007.07.011 (2008).
19. Noriega, C. & Araujo, M. Carbon dioxide emissions from estuaries of northern and northeastern Brazil. *Sci. Rep*. **4**, 10.1038/srep06164 (2014).
20. Frankignoulle, M., Bourge, I. & Wollast, R. Atmospheric CO2 fluxes in a highly polluted estuary (the Scheldt). *Limnol. Oceanogr.* **41**, 365–369 (1996).
21. Neal, C., House, W. A., Jarvie, H. P. & Eatherall, A. The significance of dissolved carbon dioxide in major lowland rivers entering the North Sea. *Sci. Total Environ.* **210**, 187–203, doi:10.1016/S0048-9697(98)00012-6 (1998).
22. Ortega, T., Ponce, R., Forja, J. & Gomez-Parra, A. Fluxes of dissolved inorganic carbon in three estuarine systems of the Cantabrian Sea (north of Spain). *J. Marine Syst.* **53**, 125–142, doi:10.1016/j.marsys.2004.06.006 (2005).
23. Richey, J. E., Melack, J. M., Aufdenkampe, A. K., Ballester, V. M. & Hess, L. L. Outgassing from Amazonian rivers and wetlands as a large tropical source of atmospheric CO2. *Nature* **416**, 617–620, doi:10.1038/416617a (2002).
24. Jones, J. B. & Mulholland, P. J. Carbon dioxide variation in a hardwood forest stream: An integrative measure of whole catchment soil respiration. *Ecosystems* **1**, 183–196 (1998).
25. Cole, J. J. & Caraco, N. F. Carbon in catchments: connecting terrestrial carbon losses with aquatic metabolism. *Mar. Freshwater Res.* **52**, 101–110, doi:10.1071/Mf00084 (2001).
26. Loder, T. C. & Reichard, R. P. The Dynamics of Conservative Mixing in Estuaries. *Estuaries* **4**, 64–69, doi:10.2307/1351543 (1981).
27. Abril, G., Etcheber, H., Delille, B., Frankignoulle, M. & Borges, A. V. Carbonate dissolution in the turbid and eutrophic Loire estuary. *Mar. Ecol. Prog. Ser.* **259**, 129–138, doi:10.3354/Meps259129 (2003).
28. Regnier, P. & Steefel, C. I. A high resolution estimate of the inorganic nitrogen flux from the Scheldt estuary to the coastal North Sea during a nitrogen-limited algal bloom, spring 1995. *Geochim. Cosmochim. Ac.* **63**, 1359–1374, doi:10.1016/S0016-7037(99)00034-4 (1999).
29. Morse, J. W., Mucci, A. & Millero, F. J. Solubility of Calcite and Aragonite in Seawater of 35-Percent Salinity at 25-Degrees-C and Atmospheric-Pressure. *Geochim. Cosmochim. Ac.* **44**, 85–94, doi:10.1016/0016-7037(80)90178-7 (1980).
30. Bouillon, S. *et al*. Inorganic and organic carbon biogeochemistry in the Gautami Godavari estuary (Andhra Pradesh, India) during pre-monsoon: The local impact of extensive mangrove forests. *Global Biogeochem. Cy.* **17**, 10.1029/2002gb002026 (2003).
31. Abril, G. *et al*. Oxic/anoxic oscillations and organic carbon mineralization in an estuarine maximum turbidity zone (The Gironde, France). *Limnol. Oceanogr.* **44**, 1304–1315 (1999).
32. Dejonge, V. N. & Villerius, L. A. Possible Role of Carbonate Dissolution in Estuarine Phosphate Dynamics. *Limnol. Oceanogr.* **34**, 332–340 (1989).
33. Pereira, P., Caçador, I., Vale, C., Caetano, M. & Costa, A. L. Decomposition of belowground marshes (Tagus litter and metal dynamics in salt Estuary, Portugal). *Sci. Total Environ.* **380**, 93–101, doi:10.1016/j.scitotenv.2007.01.056 (2007).
34. Borges, A. V. et al. Atmospheric CO2 flux from mangrove surrounding waters. *Geophys. Res. Lett.* **30**, 10.1029/2003gl017143 (2003).
35. Bouillon, S. *et al*. Importance of intertidal sediment processes and porewater exchange on the water column biogeochemistry in a pristine mangrove creek (Ras Dege, Tanzania). *Biogeosciences* **4**, 311–322 (2007).
36. Cabrita, M. T. & Brotas, V. Seasonal variation in denitrification and dissolved nitrogen fluxes in intertidal sediments of the Tagus estuary, Portugal. *Mar. Ecol-Prog. Ser.* **202**, 51–65 (2000).
37. Thomas, H. *et al*. Enhanced ocean carbon storage from anaerobic alkalinity generation in coastal sediments. *Biogeosciences* **6**, 267–274 (2009).
38. Cai, W. J., Pomeroy, L. R., Moran, M. A. & Wang, Y. C. Oxygen and carbon dioxide mass balance for the estuarine-intertidal marsh complex of five rivers in the southeastern US. *Limnol. Oceanogr.* **44**, 639–649 (1999).
39. Jiang, L. Q., Cai, W. J. & Wang, Y. C. A comparative study of carbon dioxide degassing in river- and marine-dominated estuaries. *Limnol. Oceanogr.* **53**, 2603–2615, doi:10.4319/lo.2008.53.6.2603 (2008).
40. Borges, A. *et al*. Variability of the gas transfer velocity of CO_2 in a macrotidal estuary (the Scheldt). *Estuaries* **27**, 593–603, doi:10.1007/bf02907647 (2004).
41. de la Paz, M., Gómez-Parra, A. & Forja, J. Inorganic carbon dynamic and air–water CO_2 exchange in the Guadalquivir Estuary (SW Iberian Peninsula). *J. Mar. Syst.* **68**, 265–277, doi:10.1016/j.jmarsys.2006.11.011 (2007).
42. Carini, S. *et al*. Gas exchange rates in the Parker River estuary, Massachusetts. *Biol. Bull.* **191**, 333–334 (1996).
43. Raymond, P. A. & Cole, J. J. Gas exchange in rivers and estuaries: Choosing a gas transfer velocity. *Estuaries* **24**, 312–317, doi:10.2307/1352954 (2001).
44. Cai, W. J., Wiebe, W. J., Wang, Y. C. & Sheldon, J. E. Intertidal marsh as a source of dissolved inorganic carbon and a sink of nitrate in the Satilla River-estuarine complex in the southeastern US. *Limnol. Oceanogr.* **45**, 1743–1752 (2000).
45. Abril, G., Etcheber, H., Borges, A. V. & Frankignoulle, M. Excess atmospheric carbon dioxide transported by rivers into the Scheldt estuary. *Cr. Acad. Sci. II A* **330**, 761–768, doi:10.1016/S1251-8050(00)00231-7 (2000).
46. Borges, A. V., Schiettecatte, L. S., Abril, G., Delille, B. & Gazeau, E. Carbon dioxide in European coastal waters. *Estuar. Coast. Shelf S.* **70**, 375–387, doi:10.1016/j.ecss.2006.05.046 (2006).
47. Braunschweig, F., Martins, F., Chambel, P. & Neves, R. A methodology to estimate renewal time scales in estuaries: the Tagus Estuary case. *Ocean. Dynam.* **53**, 137–145, doi:10.1007/s10236-003-0040-0 (2003).
48. Carrit, D. E. & Carpenter, J. H. Comparison and evaluation of currently employed modifications of the Winkler method for determining oxygen in seawater. *A NASCO Report.* **24**, 286–318 (1966).
49. Dickson, A. G., Sabine, C. L. & Christian, J. R. Guide to best practices for ocean CO_2 measurements. *PICES Special Publication* **3**, 191 (2007).
50. Johnson, H. K. Simple expressions for correcting wind speed data for elevation. *Coastal Engineer.* **36**, 263–269, doi:10.1016/s0378-3839(99)00016-2 (1999).
51. Conway, T. J., Lang, P. M. & Masarie, K. A. Atmospheric CO_2 data from the Terceira Island's reference station. ftp://cdiac.ornl.gov/pub/ndp005/README_flask_co2.html. Date of access:19/05/2008 (2008).
52. Hunter, K. A. The temperature dependence of pH in surface seawater. *Deep-Sea Res. Pt I* **45**, 1919–1930, doi:10.1016/s0967-0637(98)00047-8 (1998).
53. Millero, F. J., Graham, T. B., Huang, F. & Bustos-Serrano, H. & Pierrot, D. Dissociation constants of carbonic acid in seawater as a function of salinity and temperature. *Mar. Chem.* **100**, 80–94, doi:10.1016/j.marchem.2005.12.001 (2006).
54. Weiss, R. F. Carbon dioxide in water and seawater: the solubility of a non-ideal gas. *Mar. Chem.* **2**, 203–215, doi:10.1016/0304-4203(74)90015-2 (1974).

55. Kremer, J. N., Reischauer, A. & D'Avanzo, C. Estuary-specific variation in the air-water gas exchange coefficient for oxygen. *Estuaries* **26**, 829–836, doi:10.1007/Bf02803341 (2003).
56. Guerin, F. *et al.* Gas transfer velocities of CO2 and CH4 in a tropical reservoir and its river downstream. *J. Marine Syst.* **66**, 161–172, doi:10.1016/j.jmarsys.2006.03.019 (2007).
57. Clark, J. F., Simpson, H. J., Smethie, W. M. & Toles, C. Gas-Exchange in a Contaminated Estuary Inferred from Chlorofluorocarbons. *Geophys. Res. Lett.* **19**, 1133–1136, doi:10.1029/92gl00558 (1992).
58. Martins, F., Leitao, P., Silva, A. & Neves, R. 3D modelling in the Sado estuary using a new generic vertical discretization approach. *Oceanol. Acta* **24**, S51–S62 (2001).
59. Oliveira, A., Mateus, M., Cabecadas, G. & Neves, R. Water-air CO2 fluxes in the Tagus estuary plume (Portugal) during two distinct winter episodes. *Carbon Bal. Manag.* **10**, 2 (2015).
60. Mateus, M., Vaz, N. & Neves, R. A process-oriented model of pelagic biogeochemistry for marine systems. Part II: Application to a mesotidal estuary. *J. Marine Syst.* **94**, S90–S101, doi:10.1016/j.jmarsys.2011.11.009 (2012).

Acknowledgements

This work was supported by the European Commission, Programa POPesca MARE Project 22–05–01-FDR-0015 and by FCT/MCTES (PIDDAC) through project UID/EEA/50009/2013. Support was also provided to A.P. Oliveira Ph.D studies by the Portuguese Science Foundation (FCT), contract SFRH/BD/28507/06. The work of M. Mateus was partially supported by Project BioPlume - Dependence of coastal ecosystems on river run-off: today & tomorrow (PTDC/AAG-REC/2139/2012), funded by FCT and by FCT/MCTES (PIDDAC) through project UID/EEA/50009/2013. We would like to extend our gratitude to IPMA - Laboratório de Oceanografia Química team members for sampling, technical and analytical assistance.

Author Contributions

A.P.O. was responsible for the field work and M.D.M. was responsible for the simulations using MOHID. All authors wrote the main manuscript text. All authors reviewed the manuscript.

Additional Information

Competing Interests: The authors declare that they have no competing interests.

Publisher's note: Springer Nature remains neutral with regard to jurisdictional claims in published maps and institutional affiliations.